

A.C.C. Sips, J. Schweinzer, G. Jackson, S. Wolfe, J. Hobirk, H. Hoehnle,  
A. Hubbard, E. Joffrin, C. Kessel, P. Lomas, T.C. Luce, E. de la Luna,  
I. Nunes, J. Stober, the ASDEX-Upgrade team, the DIII-D team,  
the C-Mod team, the Integrated Operation Scenario Topical Group of the ITPA  
and JET EFDA contributors

# Demonstrating the ITER baseline operation at $q_{95}=3$



# Demonstrating the ITER baseline operation at $q_{95}=3$

A.C.C. Sips<sup>1,2</sup>, J. Schweinzer<sup>3</sup>, G. Jackson<sup>4</sup>, S. Wolfe<sup>5</sup>, J. Hobirk<sup>3</sup>, H. Hoehnle<sup>6</sup>,  
A. Hubbard<sup>5</sup>, E. Joffrin<sup>7</sup>, C. Kessel<sup>8</sup>, P. Lomas<sup>9</sup>, T.C. Luce<sup>4</sup>, E. de la Luna<sup>10</sup>, I.  
Nunes<sup>11</sup>, J. Stober<sup>3</sup>, the ASDEX-Upgrade team\*, the DIII-D team\*, the C-Mod  
team\* and the Integrated Operation Scenario Topical Group of the ITPA  
and JET EFDA contributors\*

*JET-EFDA, Culham Science Centre, OX14 3DB, Abingdon, UK*

<sup>1</sup> *JET-EFDA, Culham Science Centre, Abingdon OX14 3DB, UK.*

<sup>2</sup> *European Commission, Brussels, Belgium.*

<sup>3</sup> *Max-Planck-Institut für Plasmaphysik, EURATOM-Association, D-85748, Garching, Germany.*

<sup>4</sup> *General Atomics, San Diego, USA.*

<sup>5</sup> *Massachusetts Institute of Technology, Plasma Science and Fusion Center, Cambridge, USA.*

<sup>6</sup> *Institut für Plasmaphysik, University Stuttgart, D-70569 Stuttgart, Germany.*

<sup>7</sup> *Association Euratom-CEA, Cadarache 13108 Saint Paul Lez Durance, France.*

<sup>8</sup> *Plasma Physics Laboratory, Princeton University, Princeton, USA.*

<sup>9</sup> *EURATOM/UKAEA Fusion Association, Culham Science Centre, Abingdon OX14 3DB, UK.*

<sup>10</sup> *Laboratorio Nacional de Fusion, Asociacion EURATOM-CIEMAT, Madrid, Spain*

<sup>11</sup> *Euratom/IST Fusion Association, Centro de Fusao Nuclear, Lisboa, Portugal.*

\* *See Appendix of Stroth U. et al 2012, 24th IAEA FEC, OV/2-2*

\* *See the Appendix of Hill d. et al 2012, 24th IAEA FEC, OV/1-1*

† *See the Appendix of Greenwald M. et al 2012, 24th IAEA FEC, OV/2-3*

\* *See annex of F. Romanelli et al, "Overview of JET Results",  
(24th IAEA Fusion Energy Conference, San Diego, USA (2012)).*

Preprint of Paper to be submitted for publication in Proceedings of the  
24th IAEA Fusion Energy Conference (FEC2012), San Diego, USA

8th October 2012 - 13th October 2012

“This document is intended for publication in the open literature. It is made available on the understanding that it may not be further circulated and extracts or references may not be published prior to publication of the original when applicable, or without the consent of the Publications Officer, EFDA, Culham Science Centre, Abingdon, Oxon, OX14 3DB, UK.”

“Enquiries about Copyright and reproduction should be addressed to the Publications Officer, EFDA, Culham Science Centre, Abingdon, Oxon, OX14 3DB, UK.”

The contents of this preprint and all other JET EFDA Preprints and Conference Papers are available to view online free at [www.iop.org/Jet](http://www.iop.org/Jet). This site has full search facilities and e-mail alert options. The diagrams contained within the PDFs on this site are hyperlinked from the year 1996 onwards.

## ABSTRACT

In ITER, H-mode operation at 15MA and  $q_{95}=3$  is planned to achieve  $Q=10$  in deuterium-tritium mixtures. The Integrated Operation Scenario Topical Group of the ITPA has coordinated experiments in ASDEX Upgrade (AUG), Alcator C-Mod (C-Mod), DIII-D and JET to obtain H-mode data at  $q_{95}\sim 3$ . New databases have been generated for AUG and JET, using only data with the carbon wall at JET. The data span a wide range of operating conditions at  $q_{95}\sim 3$ , from discharges close to the H-mode threshold power ( $P_{LH}$ ) to H-modes at high input power ( $P_{in}/P_{LH}=4-5$ ). H-modes close to  $P_{LH}$  can achieve  $H_{98}\sim 1$  and  $f_{GW}>0.8$ . However, at JET this is obtained at low ELM frequency, with  $f_{ELM}<10\text{Hz}$  for  $P_{in}/P_{LH}<1.1$ . At higher  $P_{in}/P_{LH}\geq 2$ , the bulk of the data achieve  $H_{98}\sim 1$ , with the maximum achievable  $H_{98}$  factor increasing to 1.2. RF power has been used in ELMing H-modes providing up to 60% of the total input power in AUG and up to 20% in JET, giving similar results compared to NB only discharges. In AUG, the use of RF has beneficial effects for achieving stationary discharges with the full W wall. Only C-Mod has 100% ICRF heated H-mode data at ITER relevant parameters and  $q_{95}\sim 3$ . A range of densities has been explored. High normalised density,  $f_{GW}>0.8$ , can be obtained at low input power in AUG and JET. At higher input powers and increasing  $P_{in}/P_{LH}\geq 2$  however, the maximum achievable  $f_{GW}$  decreases to 0.85. The experiments typically report a drop in the plasma inductance up to  $l_i(3)\sim 0.7$  with increasing plasma beta up to  $\beta_N\sim 2.5$ . The maximum achievable  $H_{98}$  increases with beta. At high  $\beta_N>2.5$ , discharges at  $q_{95}\sim 3$  in DIII-D and AUG reach  $H_{98}=1.4-1.5$ , similar to hybrid regimes at  $q_{95}\sim 4$ . A remarkable similarity is observed in the data from the various devices for baseline H-modes at  $q_{95}\sim 3$ , giving confidence in projecting results to ITER.

## 1. INTRODUCTION

ITER requires robust operation of various plasma scenarios within the hardware constraints of the device. Operation in H-mode at 15MA and  $q_{95}=3$  is planned to achieve 500MW fusion power at  $Q=10$  with confinement enhancement factor  $H_{98}=1$  and plasma densities at 0.85 of the Greenwald density limit ( $f_{GW}$ ) [1]. According to the IPB98(y,2) confinement scaling, operation below 15MA, but at fixed  $f_{GW}$ , would reduce the stored energy of the D-T plasma, more than linearly with plasma current,  $I_p^{1.34}$  [2]. Moreover, the reduction in stored energy would reduce the fusion power, and heating of the plasma, further reducing the stored energy by  $P_{in}^{0.61}$ , with  $P_{in}$  the total input power to the plasma. The effect of plasma current variations are summarised in Table I; the plasma performance, computed using  $H_{98}=1.0$  and  $f_{GW}=0.85$ , are shown for  $I_p=15\text{MA}$  (reference point),  $I_p=13.5\text{MA}$  and  $I_p=16.5\text{MA}$ . The fusion gain,  $Q$ , would drop to 6.3 at  $I_p=13.5\text{MA}$  ( $q_{95}=3.33$ ), unless the confinement is increased to  $H_{98}=1.15$ . If operation just above  $I_p=16.5\text{MA}$  ( $q_{95}=2.73$ ) can be obtained,  $Q$  would rise to nearly 16 for  $H_{98}=1.0$ , alternatively a fusion power of 500MW can be obtained with  $H_{98}=0.88$ .

The Integrated Operation Scenario Topical Group of the ITPA has coordinated experiments in Alcator C-Mod (C-Mod), ASDEX Upgrade (AUG), DIII-D and JET to obtain a dataset for assessing

H-mode scenarios at  $q_{95} \sim 3$ . Important is that data are taken for plasma operation near  $q_{95} \sim 3$ , as trends observed at different (mainly higher)  $q_{95}$  would need to be confirmed for the operation domain planned for ITER. Validation of the ITER scenario reported in the period 2008-2010 showed that plasma breakdown at ITER values for  $E_{\text{axis}} < 0.23-0.33 \text{ V/m}$  is possible and that for the current ramp up, good control of the plasma inductance is obtained using a full bore plasma shape with early X-point formation [3][4] Additional heating during the current rise phase can keep the plasma inductance  $I_i(3) < 0.85$  while H-mode transition is possible. More recently, joint experiments are aimed at demonstrating and documenting flat top operation at  $q_{95} = 3$  and  $\beta_N = 1.8$ . This paper reports on the results of these experiments, the experimental conditions, the databases used for comparisons, the access to good quality H-modes, the use of RF heating, the operation at various plasma densities and the range in plasma beta achieved. The results from DIII-D have been published before [5] and the results from C-Mod are published in an accompanying paper [6]. Hence, this paper concentrates on comparing AUG results with data from JET.

## 2. EXPERIMENTS AT $q_{95} \sim 3$

Four devices, C-Mod, AUG, DIII-D and JET have performed dedicated experiments in stationary conditions with the aim of establishing coherent results for discharges at  $q_{95} \sim 3$ ,  $\beta_N \sim 1.8$  and  $n_e \leq 0.85 n_{\text{GW}}$ . Each device operated at a range of plasma currents, a range of heating powers and operating densities.

Alcator C-Mod has operated with a Mo first wall at  $q_{95} = 3-3.2$ , matching the plasma shape proposed for ITER at  $I_p = 1.3 \text{ MA}$  and  $I_p = 0.65 \text{ MA}$  with  $B_T = 5.3 \text{ T}$  and  $B_T = 2.7 \text{ T}$  respectively. Discharges at  $I_p = 0.65 \text{ MA}$  use 2<sup>nd</sup> harmonic ICRF heating at 80GHz with up to 5MW coupled power, discharges at the highest input power use neon seeding. Operation at  $B_T = 2.7 \text{ T}$  and elongation  $\kappa \sim 1.75$  allows simultaneous access to  $\beta_N < 2.1$ ,  $H_{98} = 0.8-0.95$  and  $f_{\text{GW}} < 0.79$ . High  $\beta_N$  discharges have sometimes small ELMs in addition to EDA H-mode activity. A detailed report of the results is given in [6].

AUG has operated with a carbon wall and full tungsten wall with plasma currents in the range 0.8-1.2MA with the majority of the data obtained at  $B_T$  in the range 1.7-2.1T. Recently, and with the full tungsten wall, AUG performed several discharges at  $q_{95} = 3$  [7] at 1.1MA/1.8T using ECRH at 140GHz in X3 mode. Discharges at 1.2MA/2T used ICRH at 30MHz with the newly installed boron-coated RF protection limiter tiles. As shown in Fig. 1, stable H-mode operation with good confinement ( $H_{98} = 1.01$ ) was obtained at  $q_{95} = 3.14$  using deuterium gas dosing, achieving  $\beta_N = 1.96$ . These discharges are at medium triangularity ( $\delta_u = 0.26$ ,  $\delta_l = 0.43$ ) and reach  $f_{\text{GW}} = 0.79$ . So far, no nitrogen seeding was used in discharges at  $q_{95} \sim 3$  to obtain  $H_{98}$  slightly above 1, as reported in [8].

DIII-D has performed dedicated demonstration discharges of the ITER flat top operation point at  $I_p = 1.47 \text{ MA}$  and  $B_T = 1.92 \text{ T}$ , matching the ITER plasma shape, with  $q_{95} = 3.1$  [5]. The discharge reported in [5] achieved  $H_{98} = 1.1$ ,  $\beta_N = 1.8$  with  $f_{\text{GW}}$  slowly rising to 0.65, using 4-4.4MW NBI heating. Long pulse operation was demonstrated with stationary discharges exceeding 10 resistive timescales. The most stable discharges operate at  $\beta_N \sim 2$ , which is slightly above the ITER reference

point of  $\beta_N=1.8$ .

JET operated over a wide range of plasma currents  $I_p=1.4-4.5\text{MA}$ , with the carbon wall up to 2010. The bulk of the JET data comes from physics experiments at  $q_{95}$  near 3, rather than dedicated demonstration ITER discharges aimed at matching the current rise phase and the flat top phase proposed for ITER. In these experiments up to 25MW of NBI heating was used and up to 3.6MW ICRH, achieving a wide range of  $H_{98}=0.6-1.2$ , for  $\beta_N=0.5-2.4$  and  $f_{GW}=0.25-1.1$ . Predominately, two types of plasma shapes have been used for the experiments; at  $\delta_u\sim 0.2$ ,  $\delta_l\sim 0.33$  and at higher triangularity,  $\delta_u\sim 0.4$  and  $\delta_l\sim 0.4$ . Examples of two H-mode discharges at low and high triangularity are shown in Fig. 2. Scenario development has recently started with the ITER-like wall [9]; however, in this paper we only present a summary of the results with the carbon wall.

### 3. NEW SCALAR DATABASES FROM JET AND AUG AT Q95~3

To analyse the data available, DIII-D, JET and AUG have produced databases for operation at low  $q_{95}$ . DIII-D has used the data of  $\sim 100$  demonstration discharges to study the MHD stability of long pulse operation at  $q_{95}=2.9-3.5$  as published in [10]. Both AUG and JET have produced databases of heated discharges for  $q_{95}$  in the range 2.7-3.3. The scalar data are averaged for the time period when the stored energy is above 85% of the maximum stored energy. The AUG data (200 discharges) cover experiments over a period of more than 10 years, from a carbon wall, with increasing W coverage of the first wall to including recent experiments with the full tungsten wall. The JET data (456 discharges) have been taken from experiments with the carbon wall in 2008 and 2009 and are labelled in the figures as JET(CFC). The data obtained recently with the ITER-Like Wall for the baseline H-mode are still being analysed and will be included in the future.

### 4. H-MODE ACCESS AND SUSTAINMENT AT LOW POWER

At the nominal ITER H-mode density,  $n_e = 1.0 \times 10^{20} \text{m}^{-3}$ , the threshold power required for H-mode is  $\sim 86\text{MW}$  in deuterium plasmas as reported in [11]. In deuterium-tritium, the predicted values of PLH can be reduced to  $\sim 65\text{MW}$ , using the scaling with ion mass number  $M$  ( $P_{LH} \propto 1/M$ ) found in JET [12]. With 400-500MW fusion power in ITER, this would give a maximum  $P_{in}/P_{LH}=1.8-2.3$ , not accounting for radiation losses.

The experiments show a wide range of power requirements for sustaining H-mode. In the DIII-D demonstration discharges [5], the H-mode was triggered at low plasma density, with  $P_{in}/P_{LH} > 1.5$ , but as the density increased during the discharge, due to the low ELM frequency,  $P_{in}/P_{LH}$  approached 1 during the H-mode phase. At JET, H-mode operation at  $P_{in}/P_{LH} \sim 1$  is possible as shown in Fig. 3, with  $H_{98} \sim 1$  for the best discharges in the database. Pure ICRF heated discharges are indicated in Fig. 3 (green circles), these are at very low plasma density ( $f_{GW} \sim 0.3$ ) with transition type ELM activity and no rise in plasma density. The NBI heated discharges have typically (very) low ELM frequency, with type I ELM frequencies  $> 10\text{Hz}$  only observed for  $P_{in}/P_{LH} > 1.3$ . The discharges with ELM frequency below 5Hz are indicated by the open symbols in Fig. 3. These discharges exhibit

irregular inter-ELM period with significant variation in time of the plasma stored energy and plasma density, as reported in [13] and [14]. An example is given in Fig. 2b. Only with gas fuelling the ELM frequency increases at  $P_{in}/P_{LH} \sim 1$ , however in these discharges both  $H_{98}$  and the plasma density are reduced. More stationary discharges are obtained at higher input power in JET. The data from the four devices show that discharges near  $q_{95} \sim 3$  only achieved regular ELMing H-modes at higher plasma beta,  $\beta_N = 2.0$ . In C-Mod,  $H_{98} \sim 1$  is obtained in stationary H-modes at high input power (3-5MW) and radiation fraction of  $\sim 0.85$  using seeding [15], in which the net input power ( $P_{net}$ ) is close to  $P_{LH}$ ,  $P_{net}/P_{LH} \sim 1$ .

The combined data from AUG and JET is shown in Fig. 4 and cover a range of  $P_{in}/P_{LH}$  up to 5. The maximum achievable confinement enhancement rises until  $P_{in}/P_{LH} = 2$ . At this heating level the bulk of the data is centred at  $H_{98} = 1$  with a maximum of  $H_{98} = 1.2$ . At very high input power, some of the AUG discharges obtain even higher confinement levels, these are reported in [16] and have properties similar to hybrid discharges typically run at  $q_{95} = 3.8-4.5$ . Also DIII-D can produce these ‘‘advanced inductive’’ discharges [5] using the recipe for hybrid operation at  $q_{95} = 3.3$ , achieving  $\beta_N = 2.8$ ,  $H_{98} = 1.5$ . Compared with the baseline scenario experiments in DIII-D, ELMs are more frequent giving good density control.

## 5. RF HEATING OF H-MODES

Dedicated experiments have been performed on the use of ion cyclotron heating and electron cyclotron heating, replacing neutral beam heating in AUG (ICRH at 2T and ECRH, using X3 heating, at 1.8T), DIII-D (ECRH) and JET (ICRH), while C-Mod provides all the data using only ICRH. Previous studies at JET observe hardly any difference in the shape of electron and ion temperature profiles replacing NBI by ICRH [17], although the rotation profile changes dramatically when the co-neutral beam is reduced to zero. This is supported by AUG data at  $q_{95} \sim 4.3$ , where the pedestal top values,  $T_e$ ,  $T_i$  and  $v_{pol}$  do not change significantly when varying the ECRH/NBI heating mix [18] [19].

For discharges with  $q_{95}$  near 3 with the full tungsten wall at AUG, the electron heating in the centre is essential for stable plasma operation as shown in Fig. 1. At AUG, ECRH powers up to 2MW and ICRH power up to 7MW were used. The highest confinement is obtained combining NBI with ICRH or ECRH heating as shown in Fig. 5, plotting  $H_{98}$  versus fraction of RF heating used in the additional heating. In JET, ICRF heating at  $q_{95} = 3$  was used with a maximum of 3.6MW. Discharges with 100% ICRH power ( $P_{RF}/P_{in} = 1$ ) are at low plasma density ( $f_{GW} < 0.25-0.4$ ) and only achieve  $\beta_N < 1.0$ . At high input power in JET, the contribution of central ICRF heating to the total input power is  $< 20\%$  and show, with the carbon wall, no significant difference compared to pure neutral beam heated discharges.

## 6. OPERATION AT VARIOUS PLASMA DENSITIES

Fuelling studies of stationary H-modes at high plasma current indicate that in some experiments

it is not possible to reach  $f_{GW} > 0.8$ . In C-Mod the density is limited to  $f_{GW} < 0.79$  for  $H_{98} > 0.8$  [6], operating in configurations matching the ITER shape. C-Mod can obtain  $f_{GW} \sim 0.9$  in unfuelled ICRF heated discharges, however in these cases  $H_{98}$  is below 0.8. At AUG  $f_{GW}$  is limited to  $\leq 0.65$  for discharges at low triangularity ( $\delta_{av} < 0.25$ , with  $\delta_{av} = (\delta_u + \delta_l)/2$ ) and cannot be increased using gas puffing. In recent experiments at  $\delta_{av} \sim 0.35$  (Fig. 1)  $f_{GW} \sim 0.8$  was obtained, although these discharges were optimised for obtaining maximum confinement (lowest gas fuelling rates). At JET, high current operation for  $I_p = 3.8-4.5$  MA ( $q_{95} = 2.7-3$ ) used extensive gas dosing to mitigate the ELMs, reducing global confinement [20]. By increasing deuterium gas dosing from unfuelled to  $1 \times 10^{22}$  electrons/s, the data from AUG and JET show that in both devices the maximum achievable  $H_{98}$  is reduced by 15-20%. Similar trends are seen at JET with the ITER-like wall, using deuterium gas dosing to reduce the tungsten influxes and ensuring high enough ELM frequency to prevent tungsten accumulation [9].

The observation that the highest  $H_{98}$  factors are at zero to low gas dosing ( $< 0.5 \times 10^{22}$  electrons/s) is not due to operation at low density. At low ELM frequency and with  $P_{in}/P_{LH}$  just above 1, low fuelling H-modes can reach  $f_{GW} \sim 1$ , as shown in Fig. 6 and with  $H_{98} \sim 1$  (Fig. 4). Moreover, the maximum achieved  $f_{GW}$  reduces with  $P_{in}/P_{LH}$ . At  $P_{in}/P_{LH} \sim 2$ , the maximum  $f_{GW}$  is only 0.85 of all discharges in the new database. This is related to an increase in ELM frequency with  $P_{in}/P_{LH}$ . Hence,  $f_{GW} = 0.85-1$  is only achieved in discharges with low frequency type I ELM activity. For comparison, results of JET discharges published in 2002 [21],[22] are shown, using the data averaging technique described in section 3. These discharges were optimised for achieving  $f_{GW} \sim 1$  at  $H_{98} \sim 1$ , including discharges at high triangularity ( $\delta_l = 0.45$ ,  $\delta_u = 0.49$ ), although some are at  $q_{95} \sim 3.4$ . Moreover, the data from 2002 do not show different trends compared to 2008-2009 data from JET;  $f_{GW} \sim 1$  is obtained at reduced type I frequency in so-called “mixed type I-type II” conditions. For JET discharges with  $q_{95}$  in the range 2.7-3.3, there is no large difference in attainable  $f_{GW}$  and  $H_{98}$  for low delta ( $\delta_{av} < 0.3$ ) and high delta discharges ( $\delta_{av} \sim 0.4$ ). This is shown in Fig. 8, where as a function of the average triangularity ( $\delta_{av}$ ) the product of  $H_{98} * f_{GW}$  is plotted. Increasing  $\delta_{av}$  from 0.2 to 0.4, both AUG and JET observe a  $< 15\%$  increase in maximum attainable  $H_{98} * f_{GW}$ , with discharges at  $\delta_{av} < 0.3$  achieving  $f_{GW}$  just below 1. For example JET #76460 (2MA/1.8T,  $q_{95} = 3.03$ ) at  $\delta_{av} = 0.27$  obtains  $\beta_N = 1.92$ ,  $f_{GW} = 0.91$ ,  $H_{98} = 1.03$  at  $P_{in}/P_{LH} = 1.51$ .

## 7. RANGE OF PLASMA BETA OBTAINED

Data analyses at DIII-D on the stability of long pulse operation at  $q_{95} \sim 3$ , shows susceptibility to  $n=1$  tearing modes, appearing at constant beta after  $> 2$  energy confinement times [10]. Neither  $\beta_N$ , nor  $l_i$  are a good measure for the stability boundary for these modes. In C-Mod, all cases with  $\beta_N > 1.5$  have tearing mode activity at  $n=2$  or  $n=3$  (but not  $n=1$ ). Data for operation at  $q_{95} = 2.7-3.3$  in JET and AUG is presented in Fig. 9. The operational space in the  $l_i(3)-\beta_N$  plane is identical for JET and AUG. Both devices observe tearing modes in some discharges, with confinement reduced by (3,2) NTMs. However, no significant  $n=1$  tearing activity for the duration of the discharges has

been observed. As mentioned before, JET has data of pure ICRF heated discharges (green symbols). These are at very low plasma density ( $f_{GW} \sim 0.3$ ) with transition type ELM activity and no rise in plasma density that do not follow the trends of other H-modes ( $I_i(3)$  decreasing with  $\beta_N$ ). In JET, a range of  $\beta_N$  up to 2.2 can be maintained for up to 9 seconds (limited by the heating duration), while in AUG  $\beta_N$  above 2 can be maintained for 4s and above 2.5 for 2s (both limited by the heating duration). The AUG data at  $\beta_N > 2.5$  in Fig. 10, are the aforementioned discharges at  $q_{95} \sim 3$  that have similar behaviour to hybrid discharges.

A general increase of  $H_{98}$  with beta for both AUG and JET is shown Fig. 10, similar to trends observed in hybrid discharges [23][24]. The datasets from AUG and JET include a substantial power variation of the input power at otherwise fixed conditions, apparent from the large range in  $P_{in}/P_{LH}$  shown in Fig. 4 and Fig. 6. In C-Mod, higher values of  $H_{98} = 0.85-0.9$  are obtained at  $f_{GW} \sim 0.7$  for ICRF heated discharges at  $\beta_N = 1.7-2.0$  compared to discharges at lower  $\beta_N = 1.3-1.7$ , which only obtain  $H_{98} \sim 0.7$  at  $f_{GW} \sim 0.7$ .

## 8. DISCUSSION AND CONCLUSIONS

The ITER baseline scenario at  $H_{98} = 1$  requires operation with  $I_p$  near 15MA, and above 13.5MA ( $q_{95} < 3.3$ ) to ensure sufficient fusion performance. Experiments at AUG, C-Mod, DIII-D and JET have increased the available data for  $q_{95}$  in the range 2.7-3.3. Typically results obtained at  $q_{95} > 3.3$  are used for ITER baseline prediction without verification at  $q_{95} \sim 3$ . H-mode operation at input powers near the  $P_{LH}$  is possible, achieving  $H_{98} \sim 1$  and  $f_{GW} > 0.8$ . However, at JET this is obtained at low ELM frequency, with  $f_{ELM} < 10\text{Hz}$  for  $P_{in}/P_{LH} < 1.1$ . The effect of ELM pacing on  $H_{98}$  and plasma density needs to be documented, as reported in [25]. At higher  $P_{in}/P_{LH} = 2$ , the bulk of the data achieve  $H_{98} \sim 1$ , while the maximum achievable  $H_{98}$  factor increases to 1.2. For ELMing H-modes, moderate RF power has been used with  $P_{RF}/P_{in}$  up to 0.6. At AUG, the use of RF has beneficial effects by allowing stationary discharges with the full W wall. New JET results with the ITER-Like Wall need to be included in the database. Only C-Mod has data with 100% ICRH at ITER relevant parameters and  $q_{95} \sim 3$ . More data are required from AUG, DIII-D and JET at high RF power. High normalised density,  $f_{GW} > 0.85$  can be obtained in JET for both low ( $\delta_{av} \sim 0.27$ ) and high ( $\delta_{av} \sim 0.4$ ) triangularity. With increasing  $P_{in}/P_{LH}$  however, the maximum achievable  $f_{GW}$  values drop to 0.85 with increasing frequency of type I ELMs. At  $q_{95} \sim 3$  more experiments are required for documenting operation at  $f_{GW} \geq 0.85$ . The experiments typically report a drop in the plasma inductance with increasing plasma beta. The maximum achievable  $H_{98}$  increases with beta. At high  $\beta_N > 2.5$  discharges at  $q_{95} \sim 3$  in DIII-D and AUG reach  $H_{98} = 1.4-1.5$ , similar to hybrid regimes at higher  $q_{95} \sim 4$ . The data obtained for the four devices show remarkably similar behaviour for baseline H-modes, giving confidence in extrapolating results to ITER.

## ACKNOWLEDGEMENTS

This work was supported by EURATOM and carried out within the framework of the European Fusion Development Agreement. The views and opinions expressed herein do not necessarily reflect those of the European Commission or of the ITER Organisation.

## REFERENCES

- [1]. Shimada M. *et al* 2007 Progress in the ITER Physics Basis Chapter 1 Nucl. Fusion **47** S1
- [2]. Peeters A.G. *et al* 2007 Nuclear Fusion **47** 1341
- [3]. Sips A.C.C. *et al* 2007 Nuclear Fusion **47** 1485
- [4]. Kessel C.E. *et al* 2009 Nuclear Fusion **49** 085034
- [5]. Doyle E.J. *et al* 2010 Nuclear Fusion **50** 075005
- [6]. Kessel C.E. *et al* 2012, this conference, P2-02
- [7]. Stroth U. *et al* 2012, this conference, OV/2-2
- [8]. Kallenbach A. *et al* 2012, this conference, P1-28
- [9]. Joffrin E. *et al* 2012, this conference, EX/1-1
- [10]. Turco F. *et al* 2010 Nuclear Fusion **50** 095010
- [11]. Martin Y.R. *et al* 2008 Journal of Physics Conference Series **123** 012033
- [12]. Righi E. *et al* 1999 Nuclear Fusion **39** 309
- [13]. Sartori R. *et al* 2004 Plasma Physics Controlled Fusion, **46** 723
- [14]. Maggi C.F. *et al* 2011 13th H-mode WS in Oxford UK
- [15]. Loarte A. *et al* 2011 Physics Plasmas **18**, 056105
- [16]. Sips A.C.C. *et al* 2007 Nuclear Fusion **47** 1485
- [17]. Sartori R. *et al* 2010 Proc. of the 23rd IAEA FEC, EXC/P8-12
- [18]. Sommer F. *et al* 2011 13th H-mode WS in Oxford UK
- [19]. Stober J. *et al* 2012 this conference, EX/1-4
- [20]. Nunes I. *et al* 2010 Proc. of the 23rd IAEA FEC, EXC/P8-03
- [21]. Sartori R. *et al* 2002 Plasma Physics Controlled Fusion **44** 1801
- [22]. Saibene G. *et al* 2002 Plasma Physics Controlled Fusion **44** 1769
- [23]. Luce T.C. *et al* 2010 Proc. of the 23rd IAEA FEC, ITR/1-5
- [24]. Maggi C.F. *et al* 2010 Nuclear Fusion **50** 025023
- [25]. De la Luna E. *et al* 2012, this conference, EX/6-1

$I_p$ [MA]	<b>15</b>	<b>13.5</b>	<b>16.5</b>
$q_{95}$	3	3.33	2.73
$f_{GW}$	0.85	0.85	0.85
$n_e \times 10^{20}(\text{m}^{-3})$	1.0	0.9	1.1
$W_{th}$ change	1.0	0.80	1.26
$\beta_N$	1.8	1.6	2.06
$P_{fus}$ (MW)	500	317	791
$P_{in}$ (MW)	150	113	208
$Q_{fus}$	10	6.33	15.8
$H_{98}$ to obtain $P_{fus} = 500\text{MW}$	1.0	1.15	0.88

Table 1: Variation of ITER baseline performance at 15MA, 13.5MA and 16.5MA. Assuming  $\beta_N = 1.8$ ,  $P_{fus} = 500\text{MW}$  and  $Q = 10$  at 15MA. IPB98(y,2) scaling with  $H_{98} = 1$  is used to compute values for 13.5MA and 16.5MA, 50MW additional heating.

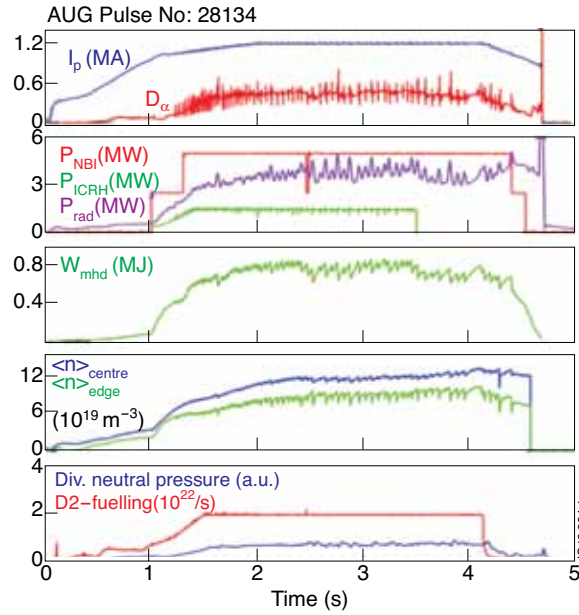


Figure 1: AUG Pulse No: 28134 (full W wall) at 1.2MA/2T at triangularity,  $\delta_{av} = 0.35$ , with ICRH at 30MHz,  $q_{95} = 3.14$ ,  $\beta_N = 1.96$ ,  $f_{GW} = 0.79$ ,  $H_{98} = 1.01$ . The discharge hits a flywheel generator I2t limit in the ramp down; the resulting stop sequence disrupts.

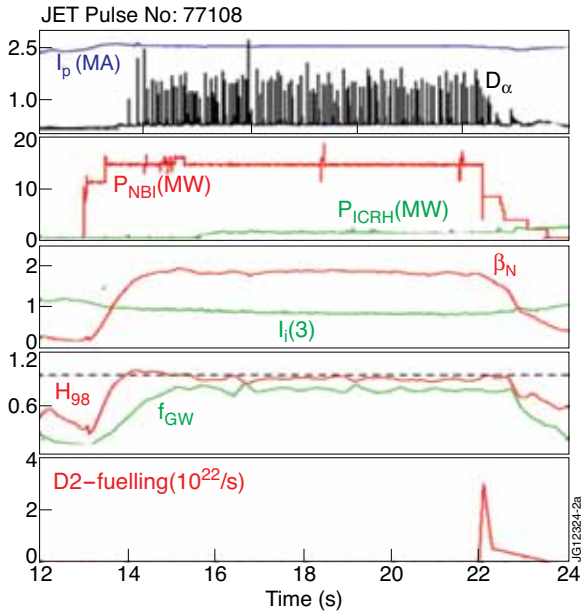


Figure 2: (a) JET with CFC walls, high delta ( $\delta_{av} = 0.43$ ).  $2.4MA/2.4T$ ,  $q_{95} = 3.28$ ,  $\beta_N = 1.77$ ,  $f_{GW} = 0.83$ ,  $H_{98} = 0.96$  and  $P_{in}/P_{LH} = 1.69$ .

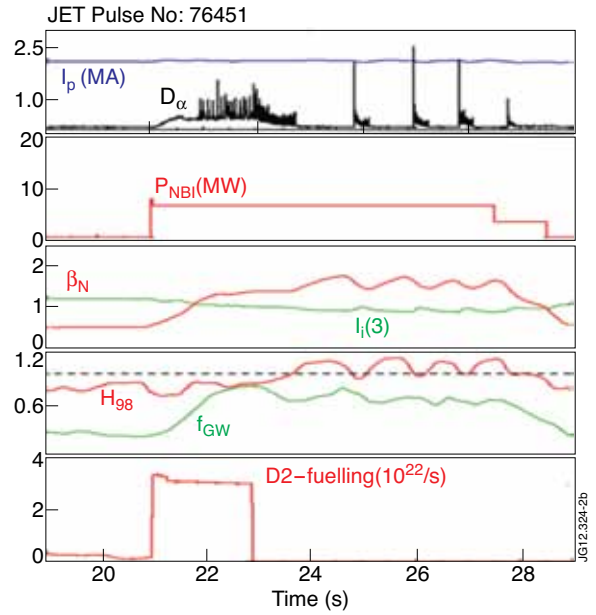


Figure 2: (b) JET with CFC walls, low delta ( $\delta_{av} = 0.25$ ).  $2MA/2T$ ,  $q_{95} = 3.25$ ,  $\beta_N = 1.52$ ,  $f_{GW} = 0.71$ ,  $H_{98} = 1.11$  and  $P_{in}/P_{LH} = 1.07$ .

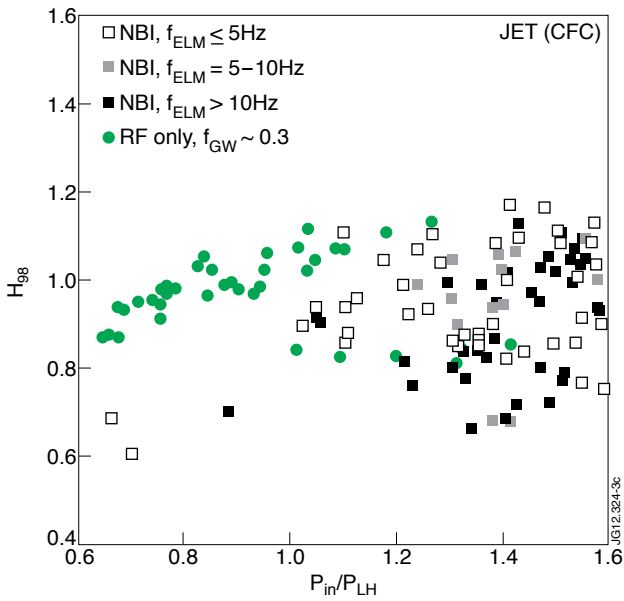


Figure 3: JET data at low input power. Discharges with ICRH only are at low density (green circles), discharges at  $f_{ELM} < 5Hz$ ,  $5-10Hz$  and  $> 10Hz$  are indicated by the open, grey and black rectangles.

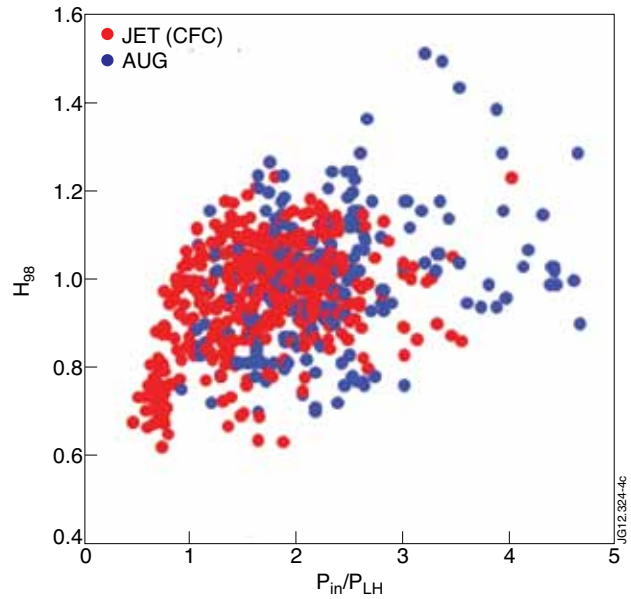


Figure 4: The confinement enhancement factor ( $H_{98}$ ) in AUG and JET for a range of  $P_{in}/P_{LH}$  up to 5.

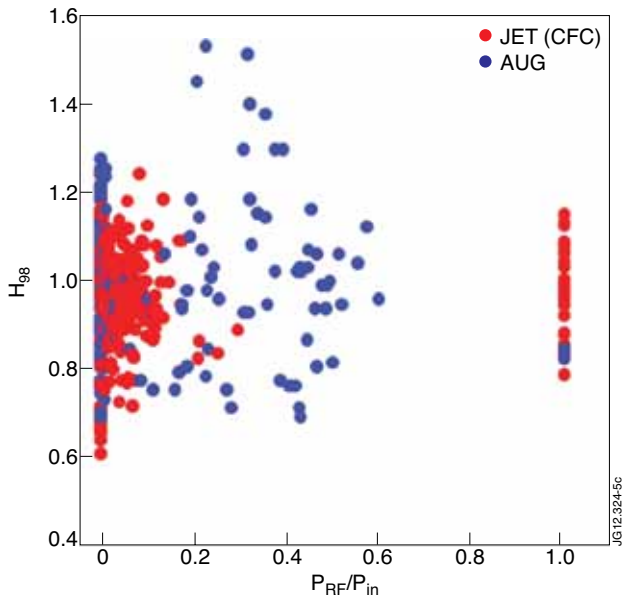


Figure 5: The confinement at AUG and JET versus contribution of RF heating to the total input power applied.

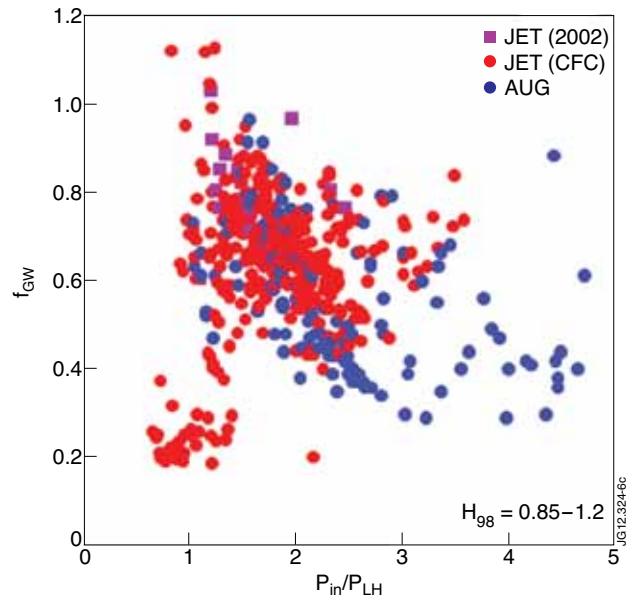


Figure 6: The normalised densities ( $f_{GW}$ ) achieved in AUG and JET for a range of  $P_{in}/P_{LH}$  up to 5, with the data restricted for  $H_{98} = 0.85-1.2$ .

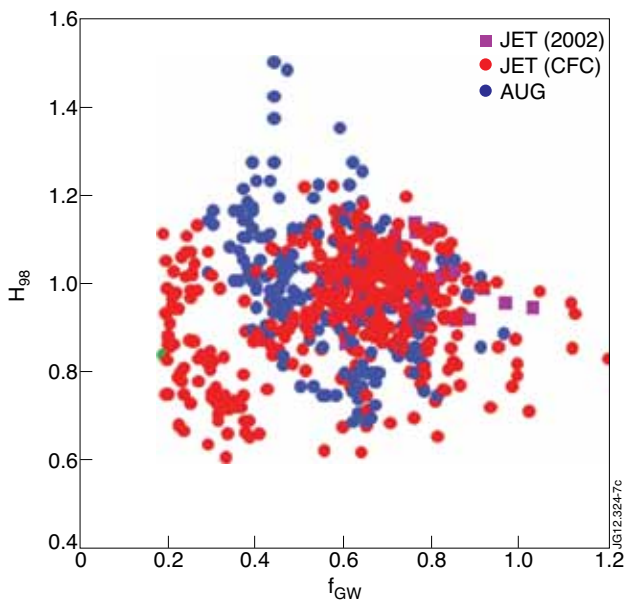


Figure 7: The confinement factor  $H_{98}$  at AUG and JET versus  $f_{GW}$ .

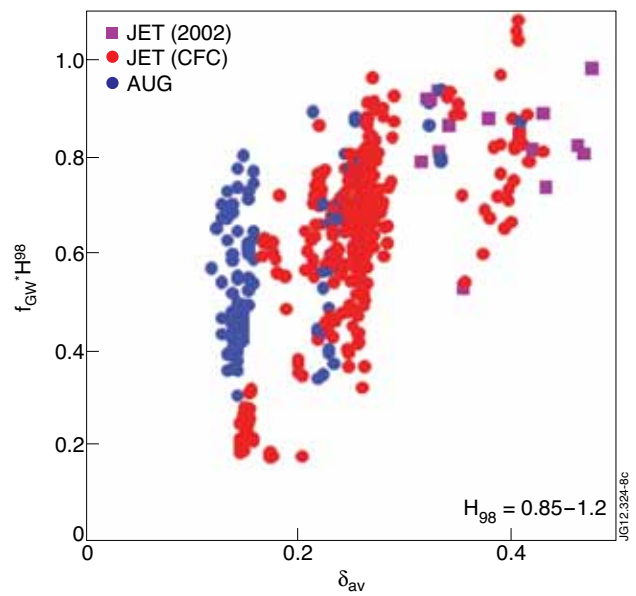


Figure 8: The product of  $f_{GW}$  and  $H_{98}$  for different triangularities ( $\delta_{av} = (\delta_u + \delta_l)/2$ ) at AUG and JET.

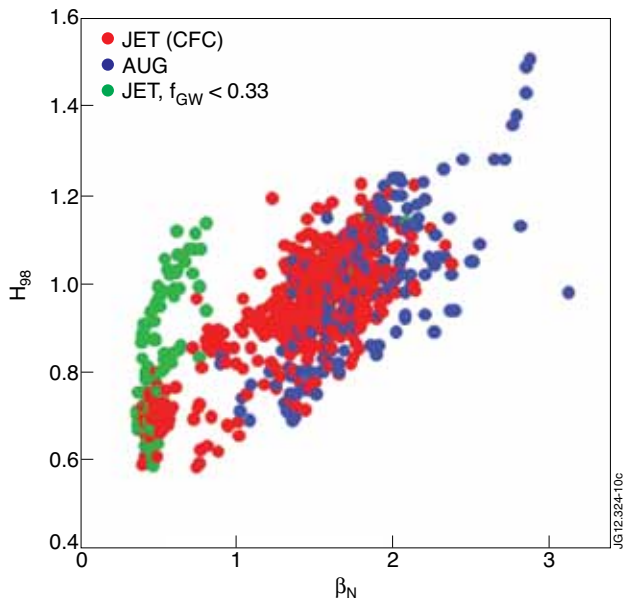


Figure 9: The variation of the normalised beta and plasma inductance for H-modes in AUG and JET.

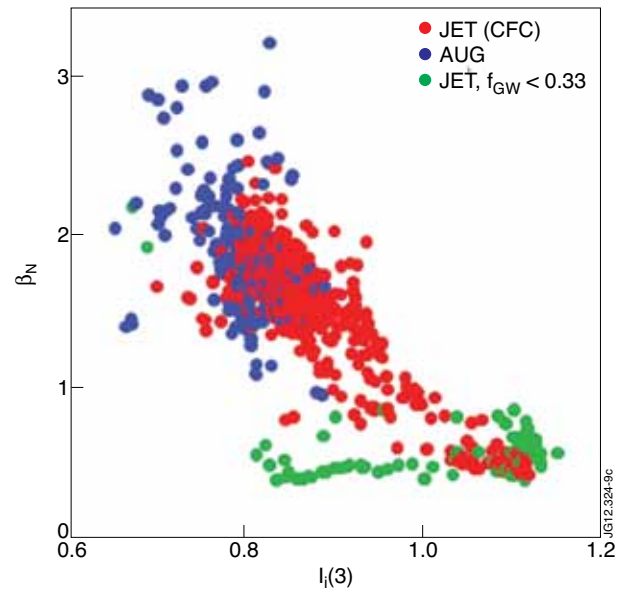


Figure 10: The increase in achievable  $H_{98}$  with normalised beta for H-modes in AUG and JET.